Analytica Chimica Acta 717 (2012) 100–109

Contents lists available at SciVerse ScienceDirect

Analytica Chimica Acta

journal homepage: www.elsevier.com/locate/aca

Multi-way partial least-squares and residual bi-linearization for the direct determination of monohydroxy-polycyclic aromatic hydrocarbons on octadecyl membranes via room-temperature fluorescence excitation emission matrices

Hector C. Goicoechea [1], Korina Calimag-Williams, Andres D. Campiglia *

Department of Chemistry, 4000 Central Florida Blvd, Physical Sciences Room 255, University of Central Florida, Orlando, FL 32816-2366, United States

ARTICLE INFO

Article history:
Received 28 July 2011
Received in revised form 8 December 2011
Accepted 15 December 2011
Available online 2 January 2012

Keywords:
Second-order multivariate calibration
Solid-phase extraction
Room-temperature fluorescence
Excitation-emission matrices
Urine analysis

ABSTRACT

Multi-way partial least-squares (N-PLS) is combined to the residual bi-linearization procedure (RBL) for the direct analysis of metabolites of polycyclic aromatic hydrocarbons in urine samples. Metabolite analysis is carried out via a two-step experimental procedure based on solid-phase extraction and room temperature fluorescence spectroscopy. Excitation-emission matrices are recorded from octadecyl (C18) membranes that serve as solid substrates for sample extraction and spectroscopic measurements. Excellent metabolite recoveries were obtained in all cases, which varied from 96.2 ± 1.35% (9-hydroxyphenanthrene) to 99.7 ± 0.49% (3-hydroxybenzo[*a*]pyrene). Background correction of extraction membranes is carried out with a new alternating least-squares (ALS) procedure adapted to second order data. The performance of N-PLS/RBL is compared to the well-established multivariate curve resolution-alternating least-squares (MCR-ALS) algorithm. Both algorithms provided similar analytical figures of merit, including their ability to handle unknown interference in urine samples. With only 10 mL of sample, the limits of detection varied between 0.06–0.08 ng mL^{-1} (1-hydroxypyrene) and 0.016–0.018 ng mL^{-1} (2-hydroxyfluorene). When compared to previously reported univariate calibration data, the limits of detection via N-PLS/RBL and MCR-ALS are approximately one order of magnitude higher. This was somehow expected due to the effect of unexpected components in multivariate figures of merit, i.e. a more realistic approach to the analysis of metabolites in human urine samples.

1. Introduction

Urine analysis of monohydroxy metabolites of polycyclic aromatic hydrocarbons (OH-PAHs) is recognized as an accurate assessment of human exposure to parent PAHs [1,2]. The general approach follows the sequence of urine hydrolysis, sample clean up and pre-concentration, and chromatographic separation and determination. The hydrolysis step is carried out to dissociate OH-PAHs from their glucuronide and/or sulfate conjugates. Popular approaches for sample clean up and pre-concentration include liquid–liquid extraction [3,4], solid-phase extraction (SPE) [5], and solid-phase micro-extraction [6]. Qualitative and quantitative analysis is usually carried out via high-performance liquid chromatography (HPLC) coupled to room-temperature fluorescence (RTF) spectroscopy [6–8] or gas chromatography–mass spectrometry (GC–MS) [9–11].

Research in our group has focused on the development of screening methodology potentially well-suited to monitor PAHs exposure of large human populations. Sample screening avoids unnecessary chromatographic analysis of negative samples, improves turnaround analysis time and reduces analysis costs. Our approach takes advantage of the strong fluorescence resulting from the rigid and delocalized π-electron system of PAHs. We have demonstrated the advantages of using SPE membranes with the dual purpose of sample pre-concentration and solid substrate for luminescence measurements [12–17]. SPE-RTF eliminates elution steps and solvent evaporation prior to metabolite determination providing excellent recoveries via a two-step procedure extremely appealing for routine analysis of numerous samples. Additional merits include compatibility with portable instrumentation for field analysis and – because of the non-destructive nature of fluorescence measurements – the possibility to bring positive samples to the lab for subsequent metabolites elution and confirmation via a high-resolution technique.

Our most recent publication extended SPE-RTF to the analysis of OH-PAHs in urine samples [18]. Its successful application was

* Corresponding author. Tel.: +1 407 823 4162; fax: +1 407 823 2252.
E-mail address: andres.campiglia@ucf.edu (A.D. Campiglia).
[1] Present address: Catedra de Quimica Analitica I, Facultad de Bioquimica y Ciencias Biologicas, Universidad Nacional del Litoral, Ciudad Universitaria, CC 242-S30001, Santa Fe, Argentina.

0003-2670/$ – see front matter © 2011 Elsevier B.V. All rights reserved.
doi:10.1016/j.aca.2011.12.031

possible with the aid of a sample holder specifically designed to improve the reproducibility of measurements on solid substrates. Background correction of extraction membranes was carried out with the aid of Asymmetric Least Squares (ALS), a smoothing algorithm originally devised for baseline correction of chromatographic data [19] and often applied to matrix interference in chromatographic analysis [20,21]. Recovery values for the studied OH-PAHs varied from 99.0 ± 1.2% (3-hydroxybenzo[a]pyrene) to 99.9 ± 0.05% (1-hydroxypyrene). The new sample holder improved the precision of measurements for analytical use. Relative standard deviations (RSD) of the studied metabolites varied from 3.5% (2-hydroxyfluorene) to 9.5% (9-hydroxyphenenthrene). The application of ALS to SPE-RTF improved the limits of detection (LOD) by approximately two orders of magnitude. With only 10 mL of urine sample, the LOD of OH-PAH varied from 57 pg mL^{-1} (2-hydroxyfluorene) to 2 pg mL^{-1} (1-hydroxypyrene) [18]. These LOD were obtained at the maximum excitation and fluorescence wavelengths of each metabolite. Their individual determination in the presence of co-existing metabolites was not attempted neither was their determination in the presence of potential fluorescence interference.

In the present article, we combine SPE to RTF excitation-emission matrix (RTF-EEM) spectroscopy and demonstrate its analytical potential with the direct determination of 2-hydroxy-fluorene (2OH-FLU), 1-hydroxy-pyrene (1OH-PYR), 3-hydroxybenzo[*a*]pyrene (3OH-B[*a*]P) and 9-hydroxy-phenanthrene (9OH-PHE) without previous chromatographic separation. Spectral overlapping of EEMs is resolved with N-PLS/RBL, a chemometric algorithm for processing second order data that combines multi-way partial least-squares (N-PLS) to the residual bi-linearization procedure (RBL) [22,23]. The performance of N-PLS/RBL is compared to the well-established multivariate curve resolution-alternating least-squares (MCR-ALS) algorithm. The analytical figures of merit obtained via a two-step experimental procedure make this approach a well-suited tool for the routine analysis of OH-PAHs in numerous samples.

Coupling multidimensional data formats – such as EEMs – with chemometric algorithms carrying the second order advantage permits the determination of calibrated species in the presence of un-calibrated concomitants, an immensely useful property in the present content. EEMs have been traditionally processed by the application of two well-known algorithms: parallel factor (PARAFAC) [24] or multivariate curve resolution-alternating least-squares (MCR-ALS) [25]. Recently attention has been paid to alternative second order multivariate calibration algorithms based on latent-structured methodologies, namely unfolded partial least squares/residual bi-linearization (U-PLS/RBL) and multidimensional partial least squares/residual bi-linearization (N-PLS/RBL) [26–28]. PLS-based methods appear to be more flexible and provide better figures of merit than their competitors [28,29]. U-PLS/RBL was recently applied in our lab to the direct analysis of OH-PAHs via a three step experimental procedure [30]. SPE was carried out on commercial C18 cartridges and PAH metabolites were directly determined in the eluting solvent (3 mL of methanol) via RTF-EEM spectroscopy. Fluorescence background reduction was achieved by flushing the SPE cartridge with 15 mL of methanol prior to sample loading. The potential interference of fluorescence concomitants typically found in urine samples was not investigated.

In the present article, we apply N-PLS/RBL to the analysis of OH-PAHs adsorbed on extraction membranes and compare its performance to the well-established MCR-ALS algorithm. Background correction of extraction membranes is carried out with a new ALS procedure adapted to second order data [31]. The crucial issue of spectral overlapping on extraction membranes was investigated with four pharmacological drugs, namely naproxen, ibuprofen, diclofenac and amoxicillin. Both N-PLS/RBL and MCR-ALS were capable to handle the presence of fluorescence interference. Their combination to SPE-RTF-EEM appears to provide a valuable approach to the routine screening of numerous samples.

2. Theory

2.1. N-PLS/RBL

Different to other second order algorithms, N-PLS/RBL includes concentration information only in the calibration step. The I calibration data arrays and the vector of calibration concentrations $\mathbf{y}$ (size $I \times 1$) are combined to generate regression coefficients $\mathbf{v}$ (size $A \times 1$) and two sets of loadings, namely $\mathbf{W}_j$ and $\mathbf{W}_k$ of sizes $J \times A$ and $K \times A$.J and K refer to digitized wavelengths in emission and excitation, respectively [32]. A is the number of latent factors, which is usually selected by leave-one-out cross-validation. In the absence of unexpected components, the analyte concentration in the test sample can be estimated with Eq. (1):

$$\mathbf{y}_u = \mathbf{t}^T\mathbf{v} \tag{1}$$

where $\mathbf{t}_u$ is the test sample score vector obtained by appropriate projection of the test data onto the calibration loading matrices.

Eq. (1) does not apply in the presence of unexpected components in the test sample. In those cases, the residuals from the N-PLS modeling of the test sample signals should be considered before making predictions. In comparison to typical instrumental noise levels, the residuals contained in the matrix $\mathbf{E}_p$ (see Eq. (2)) should be abnormally large:

$$s_p = \frac{||\mathbf{E}_p||}{(JKI - A)^{1/2}} = \frac{||\mathbf{X}_u - \text{reshape}\{\mathbf{t}_u[(\mathbf{W}_j| \otimes |\mathbf{W}_k)]\}||}{(JKI - A)^{1/2}} \tag{2}$$

In this equation, "reshape" indicates transforming a $JK \times 1$ vector into a $J \times K$ matrix and $|\otimes|$ is the Kathri–Rao operator. In order to handle the presence of unexpected constituents, residual bi-linearization resorts to the principal component analysis (PCA) of their contribution by minimizing the computed residuals while fitting the sample data to the sum of the relevant contributions. For N-PLS, the sum of contributions is given by Eq. (3):

$$\mathbf{X}_u = \text{reshape}\{\mathbf{t}_u[(\mathbf{W}_j| \otimes |\mathbf{W}_k)]\} + \mathbf{B}_{unx}\mathbf{G}_{unx}(\mathbf{C}_{unx})^T + \mathbf{E}_u \tag{3}$$

where matrices $\mathbf{B}_{unx}$, $\mathbf{G}_{unx}$ and $\mathbf{C}_{unx}$ are obtained by singular value decomposition (SVD) of the error matrix $\mathbf{E}_p$:

$$\mathbf{B}_{unx}\mathbf{G}_{unx}(\mathbf{C}_{unx})^T = \text{SVD}(\mathbf{E}_p) \tag{4}$$

During the RBL procedure, the loadings are kept constant at the calibration values, and $\mathbf{t}_u$ is varied until the final RBL residual error s_u is minimized using a Gauss–Newton procedure:

$$s_u = \frac{||\mathbf{E}_u||}{(JKI)^{1/2}} \tag{5}$$

Analyte concentrations are then obtained by introducing the values of $\mathbf{t}_u$ vectors into Eq. (1). Due to the use of PCA, retrieved RBL profiles do not necessarily resemble true spectra. The aim of RBL is to minimize the residual error term s_u to a level compatible with the degree of instrumental noise. With this in mind, one should always explore an increasing number of unexpected components and select the simplest model giving a s_u value statistically similar to the minimum.

2.2. MCR-ALS

In this algorithm, each matrix data (EEM) is unfolded in a column-wise augmented matrix $\mathbf{D}$, instead of forming a

three-dimensional data array. The bilinear decomposition of the augmented matrix **D** is carried out according to the expression:

$$\mathbf{D} = \mathbf{C} \times \mathbf{S}^{\mathrm{T}} + \mathbf{E} \quad (6)$$

where **D** rows refer to emission spectra as a function of excitation wavelengths, **C** columns contain the excitation profiles of the compounds involved in the process and the **S** columns their related emission spectra, and **E** is the matrix of residuals not fitted by the model. The appropriate dimensions of **D**, **C**, **S** and **E** are thus $K \times (1+I) \times J$, $K \times (1+I) \times F$, $J \times F$ and $K \times (1+I) \times J$ respectively (I = number of training samples, J = number of digitized emission wavelengths, F = number of extracted factors and K = number of digitized excitation wavelengths). Decomposition of **D** is achieved by iterative least-squares minimization of $||\mathbf{E}||$ under suitable constraining conditions, i.e. non-negativity in spectral profiles. It is important to keep in mind that MCR-ALS requires initialization with system parameters as close as possible to the final results. In the column-wise augmentation mode, the use of spectra is required, which should be preferentially obtained from pure analyte standards.

2.3. ALS background correction adapted to second order data

The background matrix **F** ($J \times K$) is estimated from the data matrix **M** ($J \times K$), where J and K are the number of digitized wavelengths in the emission and the excitation ranges, respectively. With this purpose, a $\mathbf{B}_1$ ($L \times J$) spline basis matrix along the rows of the **M** matrix and a $\mathbf{B}_2$ ($M \times K$) spline basis matrix along the columns of the **M** matrix are used along with a compromise of 10 basis function [33], i.e. $L = M = 10$. **F** can be represented as:

$$f_{j,k} = \sum_{L,M} b1_{LJ} b2_{MK} a_{LM} \quad (7)$$

where a_{LM} is the (L,M) element of an **A** matrix containing the regression coefficients, which can be calculated by minimizing the following cost function:

$$Q = \sum_{L,M} \nu_{JK} (y_{JK} - f_{JK})^2 + p \quad (8)$$

In Eq. (8), y is the experimental signal, f is a smooth trend (the baseline approximation), and ν are the prior weights. The elements of ν should have large values in the parts of the signal where it is allowed to affect the estimation of the baseline. Considering the choice of the following asymmetric weights: $\nu_{JK} = p$ if $\nu_{JK} > f_{JK}$ and $\nu_{JK} = 1 - p$ if $\nu_{JK} \leq f_{JK}$ with $0 < p < 1$, positive deviations from the trend will result in weights different from negative residuals. Experience shows that starting from $\nu \cong 1$, and iterating between the two computations, quickly and reliably leads to a solution in about 10 iterations. The penalty term in Eq. (8) is defined as follows:

$$p = \left[\sum_{L} \left(\Delta_1{}^{d} \mathbf{a}_{\cdot L} \right)^2 + \sum_{L} \left[\Delta_2{}^{d} \mathbf{a}_{\cdot M} \right]^2 \right] \quad (9)$$

where Δ_1 and Δ_2 are differences of order d calculated for each column ($\mathbf{a}_{\cdot L}$) and row ($\mathbf{a}_{\cdot M}$) of **A**, respectively. If different values are used for the regularization parameter Δ, the penalty may have different influence for vertical and horizontal directions.

3. Experimental

3.1. Instrumentation

Steady state excitation and fluorescence spectra and signal intensities were recorded with a commercial spectrofluorimeter (Photon Technology international). The excitation source was a continuous-wave 75-W pulsed xenon lamp with broadband illumination from 200 to 2000 nm. The excitation and emission monochromators had the same reciprocal linear dispersion (4 nm mm^{-1}) and accuracy (±1 nm with 0.25 nm resolution). The gratings were blazed at 300 and 400 nm, respectively. Detection was made with a photomultiplier tube with spectral response from 185 to 650 nm. The instrument was computer controlled using commercial software (Felix32) specifically designed for the system. Appropriate cut off filters were used to reject straight-light radiation and second-order emission.

RTF measurements were made with the aid of an in-house sample holder previously described in the literature [18]. Its design allows for the optimization of the fluorescence signal via manual rotation of its cover, which fits into the opening of the sample compartment's lid of the spectrofluorimeter. The extraction membrane is mounted on a rectangular platform and held in place by a plate with a circular window for sample excitation. Once the excitation beam is aligned with the circular window of the platform, no further optimization is needed. Maximum fluorescence intensities were observed rotating the platform to around 45° in relation to the excitation beam.

3.2. Reagents

All solvents were Aldrich HPLC grade. All chemicals were analytical-reagent grade and utilized without further purification. Unless otherwise noted, Nanopure water was used throughout. 2OH-FLU, 1OH-PYR, 9OH-PHEand naproxen were purchased from Sigma–Aldrich. 3OH-B[*a*]P was from Midwest Research Institute. All other chemicals were purchased from Fisher Chemical. The Sep-Pak C18 membranes were purchased from Varian/Agilent. The synthetic urine solution was manufactured by RICCA Chemical Company (Arlington, TX) and purchased from Fischer Scientific. Its chemical composition mimicked main components of human urine at the concentrations found in healthy urine samples.

Note: Use extreme caution when handling OH-PAH known to be extremely toxic.

3.3. Preparation of stock solutions

Stock solutions of PAH metabolites were prepared by dissolving pure standards in methanol. Naproxen, ibuprofen, diclofenac and amoxicillin stock solutions were prepared in methanol. All stock solutions were kept in the dark at 4 °C. Prior to use, stock solutions were monitored via RTF spectroscopy for possible photodegradation of metabolites. Spectral profiles and fluorescence intensities of stock solutions remained the same for a period of six months. Working solutions of OH-PAH and naproxen were prepared daily by serial dilution with methanol.

3.4. Hydrolysis of urine samples

Urine samples were spiked with micro-litters of stock solutions of appropriate concentrations and equilibrated for 30 min to allow for the interaction of metabolites and pharmaceutical drugs with urine components such as urea and various salts. Then 500 μL of 0.1 M HCl was added to the sample and the mixture was buffered with 500 μL of 0.05 M potassium biphthalate sodium hydroxide buffer (pH 5.0). The buffered sample was shaken for 30 min at 1400 rpm to allow for urine hydrolysis.

3.5. Synthetic mixtures of OH-PAHs and spiked urine samples

All metabolite concentrations were within toxicological relevant levels. Their values were adjusted to record EEM with their

true fluorescence fingerprints and fluorescence profiles with significant spectral contributions from fluorescence background and instrumental noise. Validation set #1 consisted of six synthetic mixtures (S1–S6) containing the four OH-PAHs at 2–4 ng mL^{-1} final concentrations in methanol–water (1%, v/v). Validation set #2 consisted of six urine samples (U1–U6) previously spiked with the four OH-PAHs at 2–4 ng mL^{-1} final concentrations. Validation set #3 consisted of five urine samples (UN1–UN5) previously spiked with the four OH-PAHs at the 2–4 ng mL^{-1} final concentrations and the following interferences: naproxen 200 ng mL^{-1} (UN1), ibuprofen 100 ng mL^{-1} (UN2), diclofenac 10 ng mL^{-1} (UN3), amoxicillin 50 ng mL^{-1} (UN4) and the four interferences at those final concentrations (UN5). Their concentration values matched the concentrations usually found in human urine samples.

3.6. Solid-phase extraction

A cork borer with an inside diameter of 10 mm was used to dissect a 47 mm C18 membrane into 10 mm extraction disks. A 10 mm disk was loaded into a stainless steel filter syringe kit (Alltech) and connected to a 10 mL syringe (Hamilton). Positive pressure was used to force all liquid solutions through the disk. Prior to sample application, the extraction membrane was conditioned with 5 mL of methanol and 5 mL of water. Optimization of experimental parameters concerning the retention of PAH metabolites led to the following procedure: aqueous metabolite solutions or synthetic urine samples were processed through extraction membranes previously conditioned with 5 mL methanol and 5 mL water. Following sample extraction, each membrane was sequentially rinsed with 10 mL water and 10 mL of 20% methanol/water. Void water was mechanically removed with a 100 mL syringe forcing three 100 mL volumes of air through the disk.

3.7. Software

Routines for data pre-treatment and processing were written in MATLAB [34]. Baseline routines for matrix background correction were adapted from previously reported routines for baseline correction of chromatographic data [31]. Implementation of the ALS algorithm included a smoothing parameter equal to 1×10^7, an asymmetry parameter equal to 0.005, an order of differences in penalty equal to 3 and a single regularization parameter equal to 1. MCR-ALS was applied with a graphical interface available in the literature [35]. N-PLS/RBL was implemented with an integrated chemometric toolbox (MVC2) previously currently available in the literature [36,37].

4. Results and discussion

Major attention has been paid to screening metabolites of EPA-PAHs, i.e. OH-PAHs resulting from human exposure to PAHs included in the Environmental Protection Agency (EPA) priority pollutants list. The four metabolites we chose for this study are part of this group and – as such – provide us with ample opportunity to compare our analytical figures of merit (AFOM) with previously reported data [5,8–10,38,39].

The initial survey of room-temperature excitation and fluorescence spectra on C18 membranes was carried out by extracting OH-PAHs from methanol/water (1%, v/v) solutions and hydrolyzed urine samples. All spectra were collected using 2 nm excitation and emission band-pass. No attempts were made to adjust slit widths for optimum spectral resolution, nor were the spectra corrected for instrumental response. The 2 nm band-pass provided signal-to-blank ratios higher than 3 for all the studied metabolites at the parts-per-billion (ng mL^{-1}) concentration level. Fig. 1A–D compare their spectral features recorded from C18 membranes previously used to extract methanol/water (1%, v/v) solutions. The strong overlapping that exists among the spectra of OH-PAHs prevents the direct determination of individual metabolites with a single set of excitation and fluorescence wavelengths. No significant changes were observed from spectra on C18 membranes previously used to extract hydrolyzed spiked urine samples.

Naproxen, ibuprofen, diclofenac and amoxicillin were selected to modeling the pharmacological interference that might occur in the simultaneous determination of co-extracted metabolites from urine samples of unhealthy individuals. Fig. 2 shows their excitation and fluorescence spectra recorded from C18 membranes previously used to extract standard solutions of the individual compounds in methanol/water (1%, v/v). Fluorescence spectra recorded from spiked and hydrolyzed urine samples looked virtually the same. Comparison to Fig. 1A–D confirms the strong spectral overlapping that exists with the studied metabolites.

4.1. EEM background correction of extraction membranes

The main disadvantage of SPE-RTF for quantitative analysis at trace concentration levels is the background interference from extraction membranes. The presence of broad, featureless excitation and emission bands deteriorates the LOD and often interferes with the determination of fluorescence emitters at the ng mL^{-1} concentration level. Several attempts have been made in our lab to reduce the fluorescence background of extraction membranes [18]. Because the best results were obtained via thin-layer chromatography (TLC), all further experiments in this article are carried out with extraction disks previously treated via TLC. The treatment consists of immersing membrane strips (34 mm × 40 mm) 5 mm deep in methanol three consecutive times.

Fig. 3A depicts a three-dimensional plot of the RTF-EEM recorded from an extraction membrane used to extract 10 mL of a hydrolyzed urine sample previously spiked with the four studied metabolites. The landscape corresponds to a data matrix **M** (161 × 21), which was recorded using 5 nm (excitation) and 1 nm (emission) steps. The excitation and emission wavelength ranges were selected to provide a visual comparison of the membrane background and the fluorescence signal of the metabolites mixture. The background contribution to the total fluorescence of the sample is significant within the entire wavelength ranges of the EEM. The matrix background estimation **F** (161 × 21) obtained via ALS is shown in Fig. 3B. The estimated matrix was obtained by setting L and M to a value of 10 and the asymmetry parameter (p) in Eq. (8) to 0.005. The subtraction of the **F** matrix to the **M** matrix provides the background corrected matrix shown in Fig. 3C. All further experimental EEM were background subtracted generating an ALS matrix within the excitation and emission wavelength ranges of interest.

4.2. Second order multivariate calibration

4.2.1. N-PLS/RBL

The first step in the application of N-PLS/RBL was the assessment of the optimum number of calibration factors (A). This was done by resorting to the leave-one-out cross-validation procedure, which computes the ratios $F(A) = \text{PRESS}(A < A^*)/\text{PRESS}(A)$; where PRESS is the predicted error sum of squares, defined as $\text{PRESS} = \sum (c_{i,\text{act}} - c_{i,\text{pred}})^2$, A is a trial number of factors and A^* corresponds to the minimum PRESS. The number of optimum factors was selected as the one leading to a probability of less than 75% and $F > 1$. Since the present study was carried out with four metabolites, A was equal to 4. Because the blank signal was eliminated by the pre-treatment procedure, an additional latent variable was not necessary to model the variability of the data by N-PLS.

The next step was to estimate the number of unexpected components in validation sets #2 and #3 via the post-calibration RBL

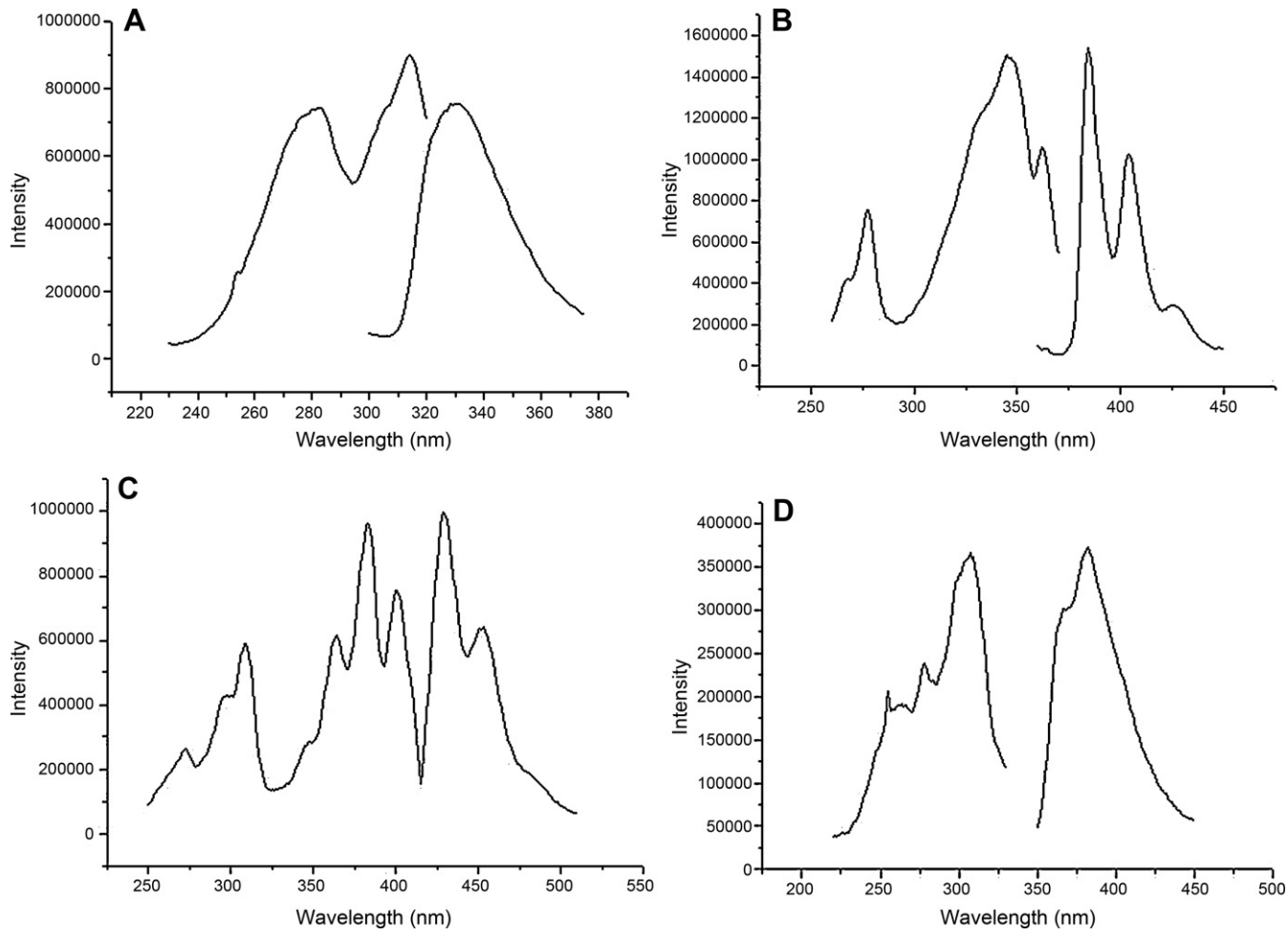

Fig. 1. Room-temperature excitation and fluorescence spectra of (A) 2OH-FLU (100 μg L^{-1}, $\lambda_{exc}/\lambda_{em}$ = 282 nm/330 nm); (B) 1OH-PYR (100 μg L^{-1}, $\lambda_{exc}/\lambda_{em}$ = 348 nm/384 nm); (C) 3OH-B[*a*]P (100 μg L^{-1}, $\lambda_{exc}/\lambda_{em}$ = 383 nm/430 nm); and (D) 9OH-PHE (100 μg L^{-1}, $\lambda_{exc}/\lambda_{em}$ = 307 nm/382 nm) on C18 membranes. Excitation and emission band-pass = 2 nm.

procedure. This was done by considering the variation of the residual (s_u) in Eq. (5) as a function of the trial number of unexpected components. The stabilization of the residual around the instrumental noise (~8.2×10^3 counts per second) suggested a single unexpected component for urine samples in the absence of naproxen and two unexpected components for samples containing naproxen. Fig. 4A and B shows the emission and excitation profiles obtained by residual bi-linearization of naproxen and a urine unknown component. The good agreement that exists among the predicted and the experimental profiles of naproxen demonstrates the success of RBL in extracting the spectral contribution of an unknown component from the sample. This ability – which refers to the second-order advantage with an accurate N-PLS algorithm – makes prediction possible with no potential interference from the sample.

After correcting the N-PLS scores of validation sets #2 and #3 with the post-calibration RBL procedure, we then applied Eq. (1) to predict the concentrations the four metabolites in all the studied samples. Table 1 compares the prediction results to the nominal concentrations of the spiked metabolites. The average recoveries for validation set #1 (S1–S6) were as follows: 2OH-FLU = 109.7 ± 19.0, 1OH-PYR = 95.5 ± 7.4, 3OH-B[*a*]P = 96.7 ± 8.7 and 9OH-PHE = 98.7 ± 11.0. Acceptable predictions were also obtained with validation set #2, i.e. urine samples in the absence of interferents (U1–U6): 2OH-FLU = 99.5 ± 10.0, 1OH-PYR = 102.7 ± 4.0, 3OH-B[*a*]P = 91.6 ± 8.0 and 9OH-PHE = 92.9 ± 9.0. Similar results were obtained with validation set #3, i.e. the urine samples (UN1–UN5) with the studied interferents: 2OH-FLU = 103.2 ± 9.1, 1OH-PYR = 100.9 ± 11.3, 3OH-B[*a*]P = 105.6 ± 9.6 and 9OH-PHE = 101.3 ± 8.7. The obtained values in the presence of interference were slightly higher than those in the absence of interference. This was somehow expected due to the strong spectral overlapping among the studied metabolites and pharmacological drugs.

Fig. 5A–C provides a visual comparison of RTF EEM recorded from S1 (synthetic metabolite mixture prepared in 1% methanol, no naproxen), U1 (synthetic metabolite mixture in urine, no naproxen) and UN1 (synthetic metabolite mixture in urine and 200 ng mL^{-1} of naproxen). Although the contribution of interferences to the total fluorescence of the sample is overwhelming, the prediction results we obtained with set #3 are within ±20% of their nominal values. This fact makes them still acceptable for validation of trace analysis in biological samples [40].

4.2.2. MCR-ALS

The MCR-ALS algorithm was applied to samples from the three validation sets. Column-wise augmented data matrices (**D**) were generated arranging $\mathbf{D}_i$ matrices corresponding to fluorescence (emission) spectra recorded in each EEM. In all cases, non-negativity was applied to both excitation and emission profiles. The number of contributions to each **D** data matrix was determined via singular value decomposition. The computed values were 4 and 5 for samples in test validation #1 and #2, respectively. For samples corresponding to set #3, 6 components were found for

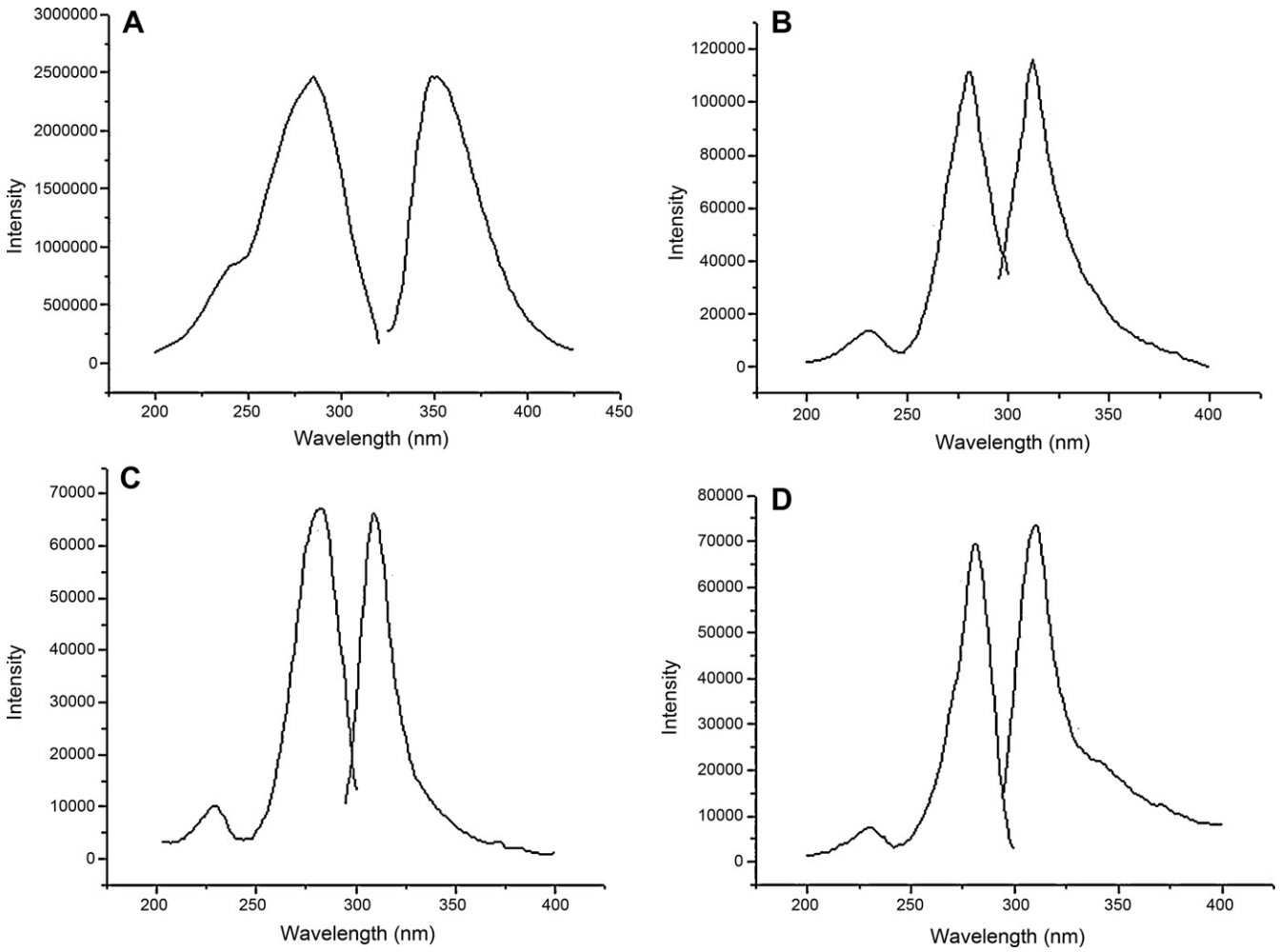

Fig. 2. Room-temperature excitation and fluorescence spectra of (A) naproxen (10 μg L^{-1}, $\lambda_{exc}/\lambda_{em}$ = 284 nm/350 nm); (B) ibuprofen (100 μg L^{-1}, $\lambda_{exc}/\lambda_{em}$ = 280 nm/308 nm); (c) diclofenac (10 μg L^{-1}, $\lambda_{exc}/\lambda_{em}$ = 282 nm/308 nm); and (D) amoxicillin (50 mg L^{-1}, $\lambda_{exc}/\lambda_{em}$ = 280 nm/310 nm) on C18 membranes. Excitation and emission band-pass = 2 nm.

Table 1
Predictions obtained when applying N-PLS/RBL to synthetic mixtures (Si), synthetic urines (Ui) and synthetic urines spiked with naproxen 200 ng mL^{-1} (UN1), ibuprofen 100 ng mL^{-1} (UN2), diclofenac 10 ng mL^{-1} (UN3), amoxicillin 50 ng mL^{-1} (UN4) and the four interferences at the previously mentioned concentrations (UN5).

Sample	2OH-FLU			1OH-PYR			3OH-B[*a*]P			9OH-PHE		
	Nominal (ng mL^{-1})	Predicted (ng mL^{-1})	Recovery (%)	Nominal (ng mL^{-1})	Predicted (ng mL^{-1})	Recovery (%)	Nominal (ng mL^{-1})	Predicted (ng mL^{-1})	Recovery (%)	Nominal (ng mL^{-1})	Predicted (ng mL^{-1})	Recovery (%)
S1	1.5	2.1 (0.1)	140.0	2.5	2.2 (0.1)	88.0	2.3	2.5 (0.1)	108.7	3.9	3.3 (0.1)	84.6
S2	2.0	2.2	110.0	2.5	2.5	100.0	2.3	2.0	87.0	2.6	2.8	107.7
S3	2.5	3.1	124.0	2.3	2.3	100.0	1.8	1.9	105.6	3.5	3.2	91.4
S4	2.3	2.2 (0.1)	95.7	2.0	1.7 (0.2)	85.0	2.2	2.0 (0.2)	90.9	3.8	3.5 (0.3)	92.1
S5	2.5	2.4	96.0	2.8	2.9	103.6	2.8	2.7	96.4	3.3	3.4	103.0
S6	2.6	2.4	92.3	2.9	2.8	96.6	2.4	2.2	91.3	3.0	3.4	113.3
U1	1.5	1.3	86.7	2.5	2.6	104.0	2.3	2.4	104.3	3.9	3.8	97.4
U2	2.0	1.9	95.0	2.5	2.6	104.0	2.3	2.0	87.0	2.6	2.8	107.7
U3	2.5	2.7	108.0	2.3	2.3	100.0	1.8	1.5	83.3	3.5	3.0	85.7
U4	2.3	2.5	108.7	2.0	2.1	105.0	2.2	1.9	86.4	3.8	3.5	92.1
U5	2.5	2.6	104.0	2.8	2.7	96.4	2.8	2.6	92.9	3.3	3.0	90.9
U6	2.6	2.3	88.5	2.9	3.1	106.9	2.4	2.3	95.8	3.0	2.5	83.3
UN1	2.5	2.6	104.0	2.3	2.0	86.9	1.8	1.6	88.9	3.2	3.3	103.1
UN2	2.5	2.7	108.0	2.3	2.5	108.9	1.8	2.0	111.1	3.2	3.5	109.4
UN3	2.5	2.2	88.0	2.3	2.4	104.3	1.8	2.0	111.1	3.2	3.0	93.8
UN4	2.5	2.6	104.0	2.3	2.1	91.3	1.8	1.9	105.6	3.2	2.9	90.6
UN5	2.5	2.8	112.0	2.3	2.6	113.0	1.8	2.0	111.1	3.2	3.5	109.4

Values between parenthesis corresponds to standard deviation for $n = 3$.

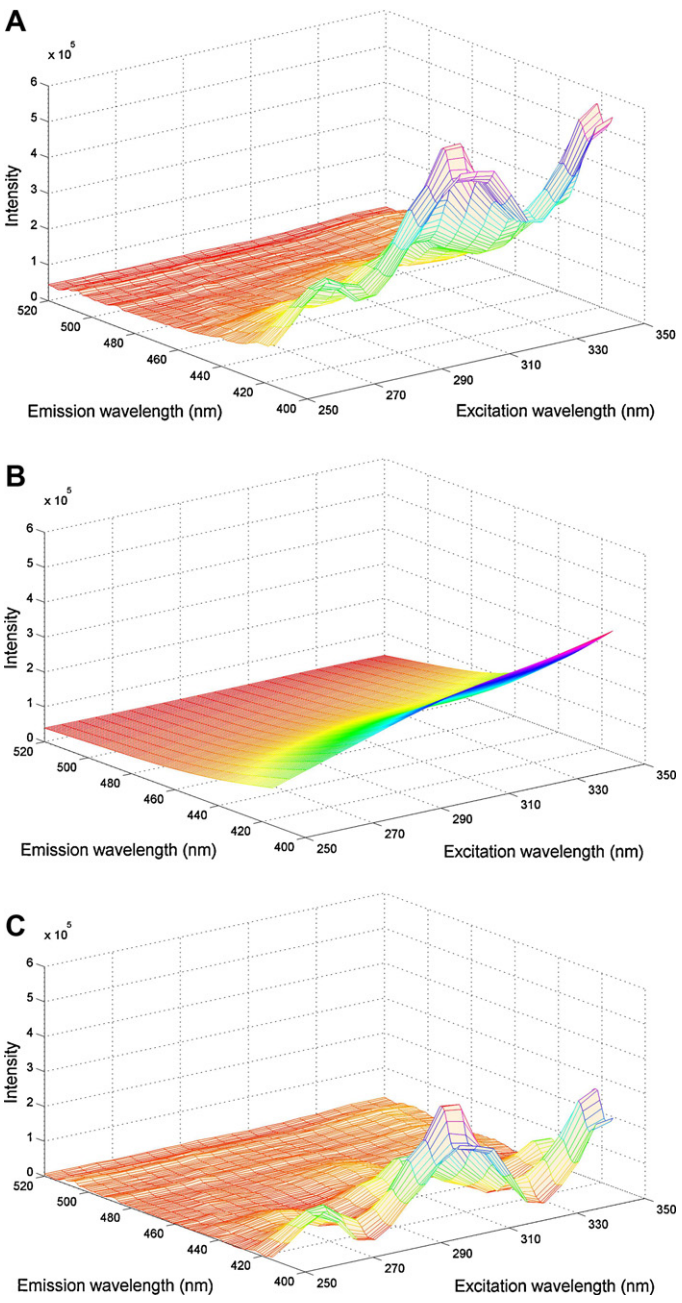

Fig. 3. (A) RTF-EEM from a C18 membrane used to extract 10 mL of hydrolyzed urine sample previously spiked with the four studied metabolites at the ng mL^{-1} concentration level. Excitation and emission steps = 5 and 1 nm, respectively. (B) Background EEM estimated via ALS. (C) EEM resulting from (A) to (B).

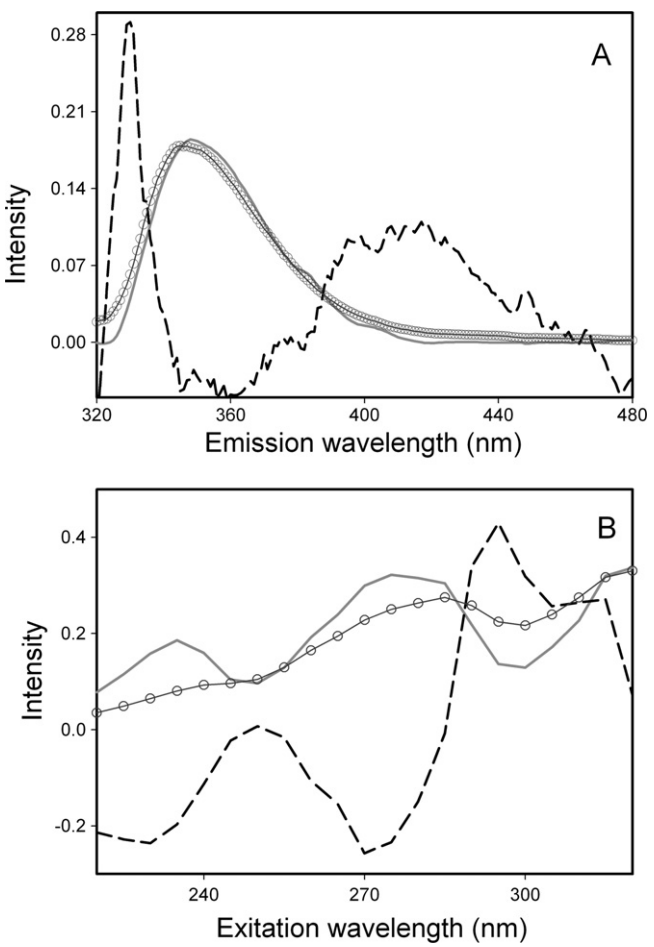

Fig. 4. Fluorescence (A) and excitation (B) profiles obtained by residual bilinearization of naproxen (solid trace; blue = predicted; red = experimental) and a urine unknown component (broken trace). Excitation and emission bandpass = 2 nm were used to record spectra. (For interpretation of the references to color in this figure legend, the reader is referred to the web version of this article.)

urines UN1–4, while for urine UN5, the number of components was 9. The $\mathbf{S}^{T}$-type initial estimates (see Eq. (6)) were built with normalized spectra from pure metabolites and – when appropriate – with random vectors for interferents. When resolution results with random estimations were unsatisfactory, the MCR spectral profiles of interferents were stored and used as initial estimations for subsequent MCR analysis until successful MCR quality parameters were reached. The effectiveness of this strategy is demonstrated in Fig. 6, which shows the MCR-ALS spectral profiles retrieved from sample UN5 containing the four studied metabolites, naproxen, ibuprofen, diclofenac, amoxicillin and an unknown urine interferent. Their visual comparison to spectra in Fig. 1 confirms the quality of the fitting and the ability to make reasonable predictions by gathering the second order advantage.

The results for the validation samples are summarized in Table 2. The average recoveries for validation set #1 (S1–S6) were as follows: 2OH-FLU = 106.5 ± 16.9, 1OH-PYR = 96.9 ± 7.0, 3OH-B[*a*]P = 97.5 ± 9.9 and 9OH-PHE = 99.7 ± 11.3. Similar predictions were obtained with urine samples (U1–U6) from validation set #2: 2OH-FLU = 99.4 ± 10.0, 1OH-PYR = 103.8 ± 6.0, 3OH-B[*a*]P = 90.6 ± 9.7 and 9OH-PHE = 94.2 ± 8.8; and with urine samples with interferents (UN1–UN5) from validation set #3: 2OH-FLU = 105.6 ± 8.8, 1OH-PYR = 98.3 ± 10.0, 3OH-B[*a*]P = 105.5 ± 5.8 and 9OH-PHE = 101.3 ± 5.7. The similarity of these averages and their standard deviations to those in Table 1 confirms the ability of N-PLS/RBL and MCR-ALS to provide equivalent results.

The accuracy of the two models was assessed by comparing the predicted to the nominal concentrations of the four metabolites in the three validation sets. The comparison was made applying the joint statistical test for the slope and the intercept of the linear regression between the nominal and predicted metabolites concentrations. The multivariate model is regarded as being accurate if the theoretical values of intercept and slope (zero and unity, respectively) are included within the ellipse that describes the mutual confidence region. In order to avoid oversizing of the joint confidence region due to the relatively large experimental random errors, as well as minimize the possibility to overlook the presence of bias and better estimate the variance of the linear regression, we included experimental data Values between

Table 2
Predictions obtained when applying MCR-ALS to synthetic mixtures (Si), synthetic urines (Ui) and synthetic urines spiked with naproxen 200 ng mL^{-1} (UN1), ibuprofen 100 ng mL^{-1} (UN2), diclofenac 10 ng mL^{-1} (UN3), amoxicillin 50 ng mL^{-1} (UN4) and the four interferences at the previously mentioned concentrations (UN5).

Sample	2OH-FLU			1OH-PYR			3OH-B[*a*]P			9OH-PHE		
	Nominal (ng mL^{-1})	Predicted (ng mL^{-1})	Recovery (%)	Nominal (ng mL^{-1})	Predicted (ng mL^{-1})	Recovery (%)	Nominal (ng mL^{-1})	Predicted (ng mL^{-1})	Recovery (%)	Nominal (ng mL^{-1})	Predicted (ng mL^{-1})	Recovery (%)
S1	1.5	2.0 (0.1)	133.3	2.5	2.3 (0.1)	92.0	2.3	2.6 (0.1)	113.0	3.9	3.4 (0.1)	87.2
S2	2.0	2.2	110.0	2.5	2.6	104.0	2.3	2.1	91.3	2.6	2.9	111.5
S3	2.5	2.9	116.0	2.3	2.2	95.7	1.8	1.9	105.6	3.5	3.1	88.6
S4	2.3	2.1 (0.1)	91.3	2.0	1.8 (0.2)	90.0	2.2	1.9 (0.2)	86.4	3.8	3.6 (0.3)	94.7
S5	2.5	2.5	100.0	2.8	3.0	107.1	2.8	2.6	92.9	3.3	3.4	103.0
S6	2.6	2.3	88.5	2.9	2.7	93.1	2.4	2.3	95.8	3.0	3.4	113.3
U1	1.5	1.4	93.3	2.5	2.6	104.0	2.3	2.4	104.3	3.9	3.6	92.3
U2	2.0	1.8	90.0	2.5	2.7	108.0	2.3	2.1	91.3	2.6	2.9	111.5
U3	2.5	2.8	112.0	2.3	2.4	104.3	1.8	1.4	77.8	3.5	3.2	91.4
U4	2.3	2.4	104.3	2.0	2.2	110.0	2.2	1.8	81.8	3.8	3.5	92.1
U5	2.5	2.7	108.0	2.8	2.6	92.9	2.8	2.7	96.4	3.3	3.0	90.9
U6	2.6	2.3	88.5	2.9	3.0	103.4	2.4	2.2	91.7	3.0	2.6	86.7
UN1	2.5	2.7	108.0	2.3	1.9	82.6	1.8	1.5	83.3	3.2	3.3	103.1
UN2	2.5	2.6	104.0	2.3	2.4	104.3	1.8	2.0	111.1	3.2	3.4	106.3
UN3	2.5	2.3	92.0	2.3	2.3	100.0	1.8	1.9	105.5	3.2	3.0	93.8
UN4	2.5	2.7	108.0	2.3	2.2	95.7	1.8	2.0	111.1	3.2	3.1	96.9
UN5	2.5	2.9	116.0	2.3	2.5	108.7	1.8	2.1	116.6	3.2	3.4	106.3

Values between parenthesis corresponds to standard deviation for $n = 3$.

parenthesis corresponds to standard deviation for $n = 3$ recorded from all the studied samples [41].

Fig. 7A and B shows prediction regions of the global data sets obtained with the N-PLS/RBL and MCR-ALS algorithms. In all the three cases and within a confidence level of 95%, both algorithms provide S and U ellipses that contain the theoretically expected values of the intercept (0) and the slope (1). The similar size of ellipses S and U associated to the similar positioning of the expected value (0,1) within the predicted regions indicates equivalent precision and accuracy for both algorithms. Interestingly, the same occurs in the presence of interferents (naproxen, diclofenac, amoxicillin and ibuprofen), i.e. in the UN ellipses. The theoretically expected value lies inside the predicted regions of both algorithms. This is an indicative of the absence of both proportional and constant errors despite the high spectral overlapping among metabolites and interferents.

4.2.3. Analytical figures of merit

All experimental data was gathered from C18 membranes used to extract hydrolyzed urine samples previously spiked with OH-PAHs. In all cases, the volume of extracted sample was 10 mL, which is a typical volume for urine analysis of OH-PAH. The mass of extracted metabolite did not surpass the nominal breakthrough mass (30 mg) of extraction membranes. RTF-EEM was recorded at 5 nm excitation steps from 220 to 360 nm. Sample excitation was carried out from longer to shorter wavelengths to reduce the risk of photo-degradation due to extensive sample excitation. Fluorescence spectra were recorded at each excitation wavelength by scanning the emission monochromator at 1 nm steps from 300 to 500 nm. All EEMs were recorded using the same excitation (2 nm) and emission (2 nm) band-pass.

Table 3 summarizes the analytical recoveries (%*R*) of the SPE-RTF method and compares the analytical figures of merit (AFOMs) calculated via MCR-ALS and N-PLS/RBL. %*R* values were calculated with the formula $\%R = (I_{BE} - I_{AE}) \times 100$, where I_{BE} and I_{AE} refer to the fluorescence intensities before and after extraction, respectively. All measurements were made at the maximum excitation and fluorescence wavelengths of each compound. Keeping in mind that the adsorption of metabolites onto the C18 membrane occurs from an aqueous based matrix (urine) and the possibility of matrix interference on the retention of OH-PAHs, we first tested their retention from standard solutions in water/water (1%, v/v) and then compared their values to the extraction of spiked urine samples. No significant difference was observed in any of the studied metabolites ($\alpha = 0.05$; $N_1 = N_2 = 3$) [42].

The estimation of the MCR-ALS AFOMs was straightforward and based on the recovery of the pure response profiles resulting from the curve resolution procedure [43]. This approach defines sensitivity (SEN_n) as the slope of the calibration curve obtained from the plot of relative fluorescence responses and standard concentrations. The analytical sensitivity (γ_n) was calculated as the ratio between the SEN_n value and the instrumental noise (s_x), which was computed from a sample of zero concentration taking into account the errors of the slope and intercept of the calibration equation [44]. The limit of detection (LOD) was calculated with the equation $LOD = 3.3\, s_x/SEN_n$.

The N-PLS/RBL sensitivity was estimated from the following unfolded PLS/RBL equations [45]:

$$SEN_n = \frac{1}{||(\mathbf{P}_{eff}{}^{+})^{T}\mathbf{v}||} \tag{10}$$

where $\mathbf{v}$ is the $(A \times 1)$ latent vector of regression coefficients for the PLS model, and $\mathbf{P}_{eff}$ is a matrix given by:

$$\mathbf{P}_{eff} = (\mathbf{P}_{c,unx} \otimes \mathbf{P}_{b,unx})^{T}\mathbf{P} \tag{11}$$

Table 3
Analytical figures of merit of OH-PAH on extraction membranes calculated with N-PLS/RBL and MCR-ALS.

Metabolite	Recovery (%)	N-PLS/RBL			MCR-ALS		
		SEN	γ^{-1} (ng mL^{-1})	LOD (ng mL^{-1})	SEN	γ^{-1} (ng mL^{-1})	LOD (ng mL^{-1})
2OH-FLU	99.2 ± 0.24	22	0.047	0.16	18	0.055	0.18
1OH-PYR	99.4 ± 1.32	59	0.018	0.06	40	0.025	0.083
3OH-B[*a*]P	99.7 ± 0.49	31	0.033	0.11	20	0.050	0.165
9OH-PHE	96.2 ± 1.35	37	0.028	0.09	25	0.040	0.132

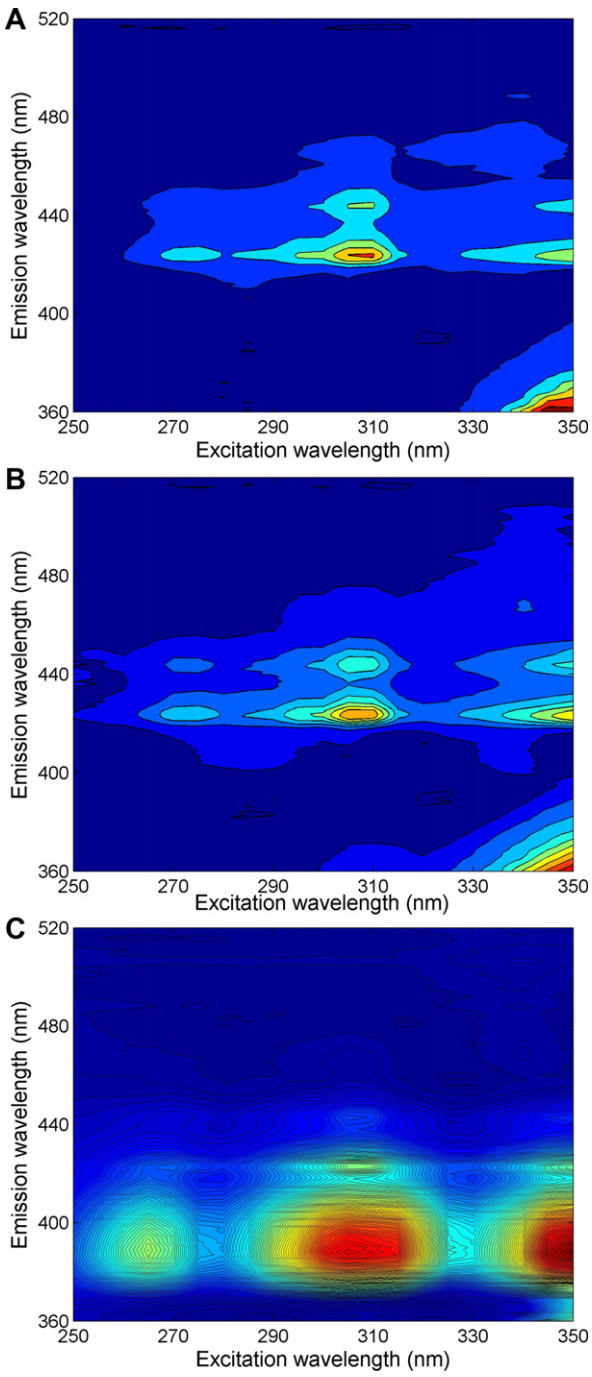

Fig. 5. RTF EEM recorded from (A) S1 (synthetic metabolite mixture prepared in 1% methanol, no naproxen); (B) U1 (synthetic metabolite mixture in urine, no naproxen); and (C) UN1 (synthetic metabolite mixture in urine and 200 ng mL^{-1} of naproxen). Excitation and emission steps = 5 and 1 nm, respectively.

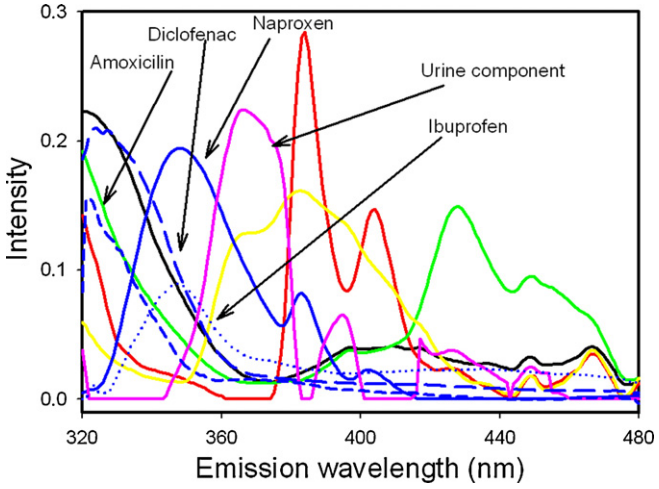

Fig. 6. MCR-ALS spectral profiles retrieved from sample UN1, which contained the four metabolites, an unknown urine interferent and naproxen. Color code as follows: 3OH-B[*a*]P = green; 9OH-Phen = yellow; 1OH-Pyr = red; 2OH-Flu = black. (For interpretation of the references to color in this figure legend, the reader is referred to the web version of this article.)

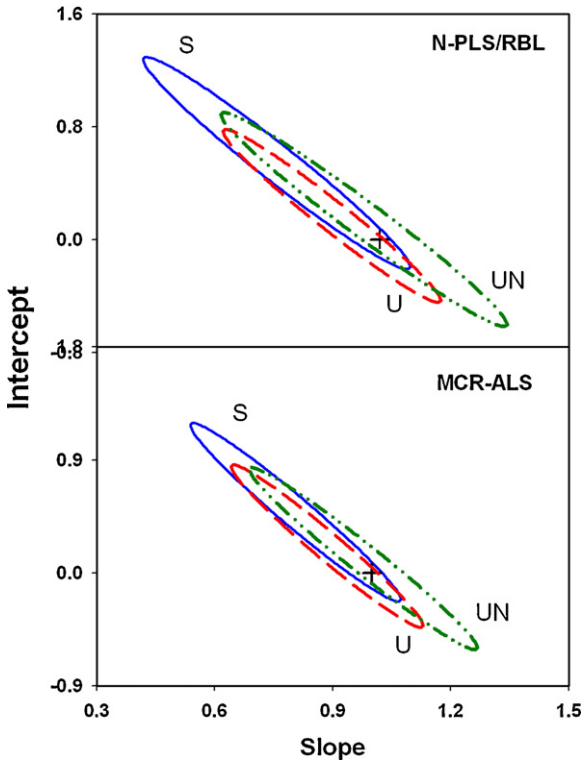

Fig. 7. Prediction regions of the global data sets obtained with (A) N-PLS/RBL and (B) MCR-ALS B algorithms.

where $\otimes$ is the Kronecker product, $\mathbf{P}$ is the $(JA \times A)$ loading matrix provided by the unfolded PLS model, and $\mathbf{P}_{c,unx}$ and $\mathbf{P}_{b,unx}$ are projection matrices calculated as follows:

$$\mathbf{P}_{c,unx} = \mathbf{I} - \mathbf{C}_{unx}\mathbf{C}_{unx}^{+} \quad (12)$$

$$\mathbf{P}_{b,unx} = \mathbf{I} - \mathbf{B}_{unx}\mathbf{B}_{unx}^{+} \quad (13)$$

where the columns of $\mathbf{B}_{unx}$ and $\mathbf{C}_{unx}$ contain the profiles of the unexpected components. The γ_n and the LOD were estimated with the same equations as those previously described for the MCR-ALS method. It is important to note that, when applying the second order advantage, the SEN_n values from Eq. (10) become sample-specific. Therefore, the results in Table 3 should be regarded as average values of the sets of samples we investigated and not as representative figures of the whole multivariate method. Although different schemes for achieving both the second-order data modeling and the AFOMs were employed, comparable results were obtained.

5. Conclusions

The direct determination of OH-PAHs on the surface of the extraction membrane makes SPE-RTF spectroscopy a well-suited

approach for screening PAH metabolites in urine samples. Its straightforward experimental procedure eliminates the need for subsequent elution steps and provides excellent metabolite recoveries. Comparison of LOD in Table 3 to previously reported univariate data [18] shows multivariate values approximately one order of magnitude higher. This was somehow predictable due to the effect of unexpected components in the multivariate figures of merit, i.e. a more realistic approach to the analysis of OH-PAH in urine samples. It should be noted that the LOD obtained with both multivariate algorithms are still comparable to those reported via HPLC methods [6–8]. Because both N-PLS/RBL and MCR-ALS are theoretically capable to handle numerous metabolites in the presence of unknown interference, their combination to SPE-RTF appears to address the crucial issue of spectral overlapping on extraction membranes.

References

[1] F.J. Jongeneelen, R.B.M. Anzion, C.M. Leijdekkers, R.P. Bos, P.T. Henderson, Int. Arch. Occup. Environ. Health 57 (1985) 47–55.
[2] F.J. Jongeneelen, R.P. Bos, R.B.M. Anzion, J.L.G. Theuws, P.T. Henderson, Scand. J. Work Environ. Health 12 (1986) 137–143.
[3] G. Grimmer, H. Brune, G. Dettarn, Arch. Toxicol. 62 (1988) 401–405.
[4] L. Yinghe, A.C. Li, H.S. Zhou, Rapid Commun. Mass Scpetrom. 19 (2005) 3331–3338.
[5] Y. Wang, W. Zhang, Y. Dong, Anal. Bioanal. Chem. 383 (2005) 804–809.
[6] G. Gmeiner, C. Krassing, E. Schmid, J. Chromatogr. B 705 (1998) 132–138.
[7] J. Gundel, J. Angerer, J. Chromatogr. B 738 (2000) 47–55.
[8] K. Kuusimaki, Y. Peltonen, P. Mutanen, Int. Arch. Occup. Environ. Health 77 (2000) 23–30.
[9] L.C. Romanoff, Z. Li, K.J. Young, J. Chromatogr. B 835 (2006) 47–54.
[10] C.J. Smith, C.J. Walcott, W. Huang, J. Chromatogr. B 778 (2000) 157–164.
[11] B. Sendar, S. Waidyanatha, Y. Zheng, Biomarkers 8 (2003) 93–109.
[12] A.F. Arruda, A.D. Campiglia, Anal. Chim. Acta 386 (1999) 271–280.
[13] E.D. Hagestuen, A.D. Campiglia, Talanta 49 (1999) 547–560.
[14] E.D. Hagestuen, A.F. Arruda, A.D. Campiglia, Talanta 52 (2000) 727–737.
[15] A.F. Arruda, A.D. Campiglia, Environ. Sci. Technol. 34 (2000) 4982–4988.
[16] J.L. Whitcomb, A.D. Campiglia, Talanta 55 (2001) 509–518.
[17] A.F. Arruda, H.C. Goicoechea, M. Santos, A.D. Campiglia, A.C. Olivieri, Environ. Sci. Technol. 37 (2003) 1385–1391.
[18] K. Calimag-Williams, H.C. Goicoechea, A.D. Campiglia, Talanta 85 (2011) 1805–1811.
[19] P.H.C. Eilers, Anal. Chem. 76 (2004) 404–411.
[20] M.M. Galera, M.D.G. Garcia, M.J. Culzoni, H.C. Goicoechea, J. Chromatogr. A 1217 (2010) 2042–2049.
[21] H.C. Goicoechea, M.J. Culzoni, M.D.G. Garcia, M.M. Calera, Talanta 83 (2011) 1098–1107.
[22] D.B. Gil, A.M. de la Peña, J.A. Aranciba, G.M. Escandar, A.C. Oliveri, Anal. Chem. 78 (2006) 8051–8058.
[23] M.J. Culzoni, H.C. Goicoechea, A.P. Pagani, M.A. Cabezon, A.C. Olivieri, Analyst 131 (2006) 718–723.
[24] R. Bro, Chemom. Intell. Lab. Syst. 38 (1997) 149–171.
[25] A. de Juan, R. Tauler, J. Chemom. 15 (2001) 749–772.
[26] S. Wold, P. Geladi, K. Esbensen, J. Øhman, J. Chemom. 1 (1987) 41–56.
[27] A.C Olivieri, J. Chemom. 19 (2005) 253–265.
[28] V.A. Lozano, G.A. Ibañez, A.C. Olivieri, Anal. Chim. Acta 651 (2009) 165–172.
[29] V.A. Lozano, G.A. Ibañez, A.C. Olivieri, Anal. Chim. Acta 610 (2008) 185–195.
[30] K. Vatsavai, H.C. Goicoechea, A.D. Campiglia, Anal. Biochem. 376 (2008) 213–220.
[31] P.H.C. Eilers, I.D. Currie, M. Durbaĭn, Comput. Stat. Data Anal. 50 (2006) 61–67.
[32] R. Bro, Multi-way analysis in the food industry, Doctoral Thesis, University of Amsterdam, Netherlands, 1998.
[33] K. Kaczmarek, B. Walczak, S. de Jong, B.G.M. Vandginste, Acta Chromatogr. 15 (2005) 82.
[34] MATLAB 7.6.0, The MathWorks, Natick, MA, USA, 2008.
[35] J. Jaumot, R. Gargallo, A. de Juan, R. Tauler, Chemom. Intell. Lab. Syst. 6 (2005) 101–110.
[36] A.C. Olivieri, W. Hai-Long, Y. Ru-Qin, Chemom. Intell. Lab. Syst. 96 (2009) 246.
[37] http://www.chemometry.com.
[38] C.T. Kuo, J. Chromatogr. B 805 (2003) 187–193.
[39] M.J. Miller, J.C. Miller, Stats. and Chemom for Anal. Chem., fourth ed., Prentice-Hall, Inc., New York, 2000.
[40] L. Huber, Guidelines for Single-laboratory Validation of Analytical Methods for Trace-level Concentrations of Organic Chemicals; Validation and Qualification in Analytical Laboratories, second ed., Informa Healthcare, New York, 2007.
[41] A. Martínez, J. Riu, O. Busto, J. Guasch, F.X. Rius, Anal. Chim. Acta 406 (2000) 257–278.
[42] J.N. Miller, J.C. Miller, Statistics and Chemometrics for Analytical Chemistry, fourth ed., Prentice Hall, New York, 2000.
[43] J. Saurina, C. Leal, R. Campañó, M. Granados, M.D. Prat, R. Tauler, Anal. Chim. Acta 432 (2001) 241–251.
[44] L.A. Currie, Anal. Chim. Acta 391 (1999) 105–126.
[45] A.C. Olivieri, J. Chemom. 19 (2005) 253–265.